AGU PUBLICATIONS

Geophysical Research Letters

RESEARCH LETTER
10.1002/2017GL074776

Key Points:
- Observation of a slow, seismic and aseismic slip sequence at the northern Hikurangi margin
- First SSE documented northeast of the North Island, New Zealand
- A long-lived transient observed north of the Hikurangi margin following the M_w 7.1

Supporting Information:
- Supporting Information S1

Correspondence to:
A. Koulali,
achraf.koulali@anu.edu.au

Citation:
Koulali, A., S. McClusky, L. Wallace, S. Allgeyer, P. Tregoning, E. D'Anastasio, and R. Benavente (2017), Slow slip events and the 2016 Te Araroa M_w 7.1 earthquake interaction: Northern Hikurangi subduction, New Zealand, *Geophys. Res. Lett.*, *44*, 8336–8344, doi:10.1002/2017GL074776.

Received 5 JUL 2017
Accepted 9 AUG 2017
Accepted article online 15 AUG 2017
Published online 31 AUG 2017

Slow slip events and the 2016 Te Araroa M_w 7.1 earthquake interaction: Northern Hikurangi subduction, New Zealand

A. Koulali[1], S. McClusky[1], L. Wallace[2,3], S. Allgeyer[1], P. Tregoning[1], E. D'Anastasio[2], and R. Benavente[4]

[1]Research School of Earth Sciences, Australian National University, Canberra, ACT, Australia, [2]GNS Science, Lower Hutt, New Zealand, [3]Institute of Geophysics, Univerity of Texas Institute for Geophysics, Austin, Texas, USA, [4]National Research Center for Integrated Natural Disaster Management, Santiago, Chile

Abstract Following a sequence of three Slow Slip Events (SSEs) on the northern Hikurangi Margin, between June 2015 and August 2016, a M_w 7.1 earthquake struck ~30 km offshore of the East Cape region in the North Island of New Zealand on the 2 September 2016 (NZ local time). The earthquake was also followed by a transient deformation event (SSE or afterslip) northeast of the North Island, closer to the earthquake source area. We use data from New Zealand's continuous Global Positioning System networks to invert for the SSE slip distribution and evolution on the Hikurangi subduction interface. Our slip inversion results show an increasing amplitude of the slow slip toward the Te Araroa earthquake foreshock and main shock area, suggesting a possible triggering of the M_w 7.1 earthquake by the later stage of the slow slip sequence. We also show that the transient deformation following the Te Araroa earthquake ruptured a portion of the Hikurangi Trench northeast of the North Island, farther north than any previously observed Hikurangi margin SSEs. Our slip inversion and the coulomb stress calculation suggest that this transient may have been induced as a response to the increase in the static coulomb stress change downdip of the rupture plane on the megathrust. These observations show the importance of considering the interaction between slow slip events, seismic, and aseismic events, not only on the same megathrust interface but also on faults within the surrounding crust.

1. Introduction

Since their discovery, slow slip events (SSEs) on subduction zones have continued to be an enigmatic mechanism of transient aseismic stress release [*Dragert et al.*, 2001; *Peng and Gomberg*, 2010; *Schwartz and Rokosky*, 2007]. Observations of these events reveal a variety of duration, recurrence, and spatial extent [*Ito et al.*, 2007; *Ozawa et al.*, 2007; *Wallace and Beavan*, 2010; *Vallée et al.*, 2013; *Radiguet et al.*, 2016; *Dixon et al.*, 2014]. Although most early studies of SSEs were focused on the deeper (>20 km) thermally controlled transition zone between the fully coupled and creeping zone, where they were first detected, recent investigations showed that such events can also occur in the shallowest portions of the subduction megathrust [*Saffer and Wallace*, 2015; *Wallace et al.*, 2016; *Araki et al.*, 2017], suggesting that these events can play a major role in the moment release budget near the trench, and may influence near-trench earthquake and tsunami generation. Therefore, a better understanding of the spatiotemporal evolution of shallow SSEs is a key element needed to inform earthquake potential and seismic and tsunami hazard assessment.

One characteristic of many shallow (<15 km deep) SSEs is their association with seismicity [*Wallace et al.*, 2012; *Vallée et al.*, 2013; *Saffer and Wallace*, 2015]. *Segall et al.* [2006] reported swarms of high-frequency earthquakes accompanying SSEs on a normal fault flanking Kilauea volcano and proposed that the increase in seismicity is well explained by an increase in stressing rate caused by the SSE. *Kato et al.* [2012] showed that a seismic swarm and slow slip transient propagated toward the initial rupture area of the 2011 M_w 9 Tohoku-Oki earthquake, potentially triggering the earthquake. These observations were supported also by numerical simulations suggesting that SSEs have the potential to trigger earthquakes [*Segall and Bradley*, 2012]. On the other hand, the role of nearby earthquakes in the occurrence and evolution of SSE themselves is not well documented in the literature. *Wallace et al.* [2014] showed that the change in stress induced by the 2013 M_w 6.3 Eketahuna earthquake arrested an ongoing nearby SSE,

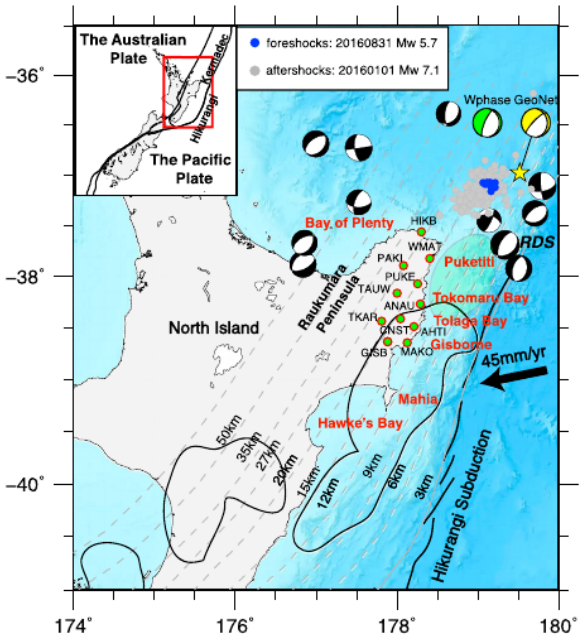

Figure 1. Regional tectonic map of the North Island (New Zealand). Major tectonic boundaries (inset) are in black; gray circles are aftershocks of the M_w 7.1 Te Araroa earthquake ($M_w > 2$ and 1 day); blue circles are the 1 day foreshocks (1 September NZ time). Dashed gray lines are contours of the slab geometry used in this study; Black Focal mechanisms are historical events from *Doser and Webb* [2003] ($M_w \geq 6$); yellow mechanism corresponds to the M_w 7.1 1 September 2016 (from GeoNet), and the Green mechanism is from our W-phase source inversion; green dots are the locations of the GPS stations; black contours correspond to where SSE was observed between 2002 and 2010 according to *Wallace et al.* [2012]; the green transparent contours is the area where the SSEs from the current study are focused. RDS: Ruatoria debris slide.

while in other cases earthquakes have triggered nearby SSEs [*François-Holden et al.*, 2008]. Here we document a complex sequence of shallow SSEs followed by a M_w 7.1 earthquake at the northern Hikurangi subduction margin, which is in turn followed by another transient deformation near the earthquake rupture area. This sequence offers a unique opportunity to explore the interactions between SSEs and earthquakes.

The Hikurangi subduction margin has generated more than 30 slow slip events over the last 15 years, with different durations, sizes, and nucleation depths [*Douglas et al.*, 2005; *Wallace and Beavan*, 2010; *Wallace et al.*, 2012; *Bartlow et al.*, 2014; *McCaffrey*, 2014; *Wallace et al.*, 2014, 2016]. Here we use continuous Global Positioning System (cGPS) observations to constrain the spatiotemporal evolution of an SSE sequence in 2016, and seismological observations (Figure 1), to investigate the interaction between the SSE sequence and the 2016 M_w 7.1 Te Araroa earthquake. We invert the GPS time series for the SSE transient sources and probe the first documented SSE reaching north of the Raukumara Peninsula along the Hikurangi margin.

2. Data and Methods

2.1. GPS Time Series Inversion of the 2015–2016 Hikurangi SSE Sequence

We use time series data from 21 continuous GPS sites in the GeoNet and PositioNZ network (http://www.geonet.org.nz/data/types/geodetic) located in the northeast part of the North Island, New Zealand. These are the product of the new processing strategy of GeoNet using GAMIT-GLOBK software (http://www.geonet.org.nz/data/supplementary/gnss_time_series_notes). We analyze the time series from February 2015 to August 2016 and correct the raw time series for instrumental offsets using the metadata provided by GeoNet. We have inspected the resulting time series and manually picked the times of the beginning of each SSE. Four SSEs were identified predominantly by their large east component of displacement (Figure 2), which is typical of past SSEs in this region [e.g., *Wallace and Beavan*, 2010]. The first event began in June 2015 with a maximum eastward displacement detected at the site ANAU with ~1 cm displacement. One year later, two successive events were detected in the same region near the coast of Tolaga Bay in May and June 2016. Both lasted approximately 20 days. Subsequent to the June 2016 event, large displacements were observed in late August on the eastern component of the sites CNST, ANAU, PUKE, and WMAT as well as the site HIKB located northward in Hicks Bay. This event lasted almost approximately 2 weeks and had a similar duration to previous SSEs observed at the northern Hikurangi margin [*Wallace and Beavan*, 2010]. In the middle of this late August/early September SSE, the M_w 7.1 Te Araroa earthquake occurred (2 September, NZ local time), just to the northeast of the SSE region (Figure 1).

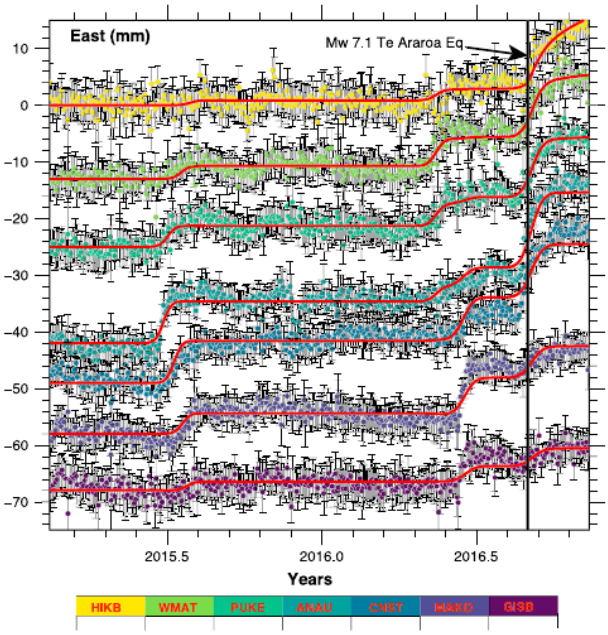

Figure 2. Daily positions time series (east component) in this study; the color code refers to stations names as labeled in the color bar; red lines show model predictions (the model shown here includes a transient on the subduction interface; and the black line refers to the date of the Te Araroa M_w 7.1 earthquake).

To gain more insight into the spatiotemporal characteristics of slip on the subduction interface during this sequence, we simultaneously invert the horizontal and vertical GPS time series for slip distribution on the Hikurangi subduction interface using TDefnode [*McCaffrey*, 2009]. This approach exploits the coherence of long-wavelength surface deformation recorded at individual stations. Instead of solving for slip at discretized patches along the fault interface, we have parametrized the slip spatial distribution using a 2-D Gaussian distribution:

$$S(x,w) = A\ \exp\left[-0.5(\mathrm{d}w/d1)^2\right] \exp\left[-0.5(\mathrm{d}x/d2)^2\right], \quad (1)$$

where $S(x,w)$ is the slip, A the amplitude, $d1$, $d2$ are the updip and downdip lengths distance from node to center of slip. The temporal evolution of the SSEs was set using a Gaussian function, with $S(t) = A\ \exp([(t - t_{\max})/T_c])$, with T_c as the time constant and $t_{\max}$as the time of the peak slip. This approach using basis functions enables us to parametrize the transient evolution with a relatively small number of free parameters, which are the slip amplitude, the along-dip and along-strike width of the zone of slip, the time constant, and the origin time of the start of the transient. In our inversion, we also estimate a migration rate and a migration azimuth, similar to the approach described by *McCaffrey* [2009]. The subduction interface geometry used is similar to *Williams et al.* [2013], discretized into a 3-D irregular grid of nodes with resolution of 25 km × 20 km. Since we are focused on the period between middle 2015 and 2016, we do not invert for locking on the subduction zone. Instead, we have inverted for a linear inter-slow slip rate simultaneously with the other transient parameters to account for the long-term trend between SSEs in the time series. The best fit parameters were obtained by simulated annealing applied to simplex minimization [*Press et al.*, 1989] that minimizes the reduced chi-square (χ^2) of the misfit to the weighed data.

2.2. Coseismic Slip Distribution of the M_w 7.1 Te Araroa Earthquake

A week after the onset of the late August 2016 SSE, an M_w 7.1 earthquake struck offshore of the north-eastern coast of New Zealand on the 2 September (NZ local time; http://www.geonet.org.nz/earthquake/2016p661332). The earthquake generated a small tsunami with ~21 cm runup height (http://ptwc.weather.gov/). The location of the epicenter was 179.52°E, 36.98°S (GeoNet catalogue; www.geonet.org.nz), northeast of the North Island. The GeoNet and the GCMT solutions show that both the main shock and many aftershocks showed well-defined normal faulting mechanisms as well as a few strike-slip events.

The timing of the earthquake with respect to the earlier SSE sequence, and the initiation of a transient event near Hicks Bay (HIKB) just after the earthquake, offers an opportunity to investigate the interaction between the two processes. To this end, a finite fault slip inversion was performed to constrain the coseismic slip distribution. As the main shock rupture was located far offshore of the East Cape, where most of cGPS stations are located, the geodetic coseismic displacements are less sensitive to the fault slip pattern. Therefore, we opted for a teleseismic inversion to retrieve the coseismic slip distribution. We used the W-phase

waveform inversion technique as described in *Benavente and Cummins* [2013]. This method has been recently used for recovering the slip pattern for moderate to large earthquakes [*Yoshimoto and Yamanaka*, 2014; *Benavente et al*., 2016].

The locations of the aftershocks do not show any specific fault geometry, and in the absence of seismic imaging near the main shock area to provide structural constraints, we rely on the focal mechanism to prescribe the fault geometry for the finite fault inversion. Thus, we have considered a coseismic fault geometry similar to the USGS preliminary solution (http://earthquake.usgs.gov/earthquakes/search/). The fault plane was divided into 19 subsegments along-strike and eight along-dip with 10 km length using a uniform dip of 26°. The synthetic waveforms produce an excellent fit to the observed displacements with a relative percent misfit (L-2 norm) of 42.2% (Figure S1 in the supporting information). The resulting slip distribution, shown in the supporting information Figure S3, indicates mostly a shallow to intermediate-depth rupture extending from the 5 to 23 km depth, with a peak of ~1 m of slip. We estimate a seismic moment of $4.5.10^{19}$ Nm (7.07 M_w) with a duration of 35 s.

3. Results and Discussion

3.1. Shallow SSEs North of Hikurangi Between 2015 and 2016

The history of North Island slow slip events over the last decade at the Hikurangi margin is distinguished by mostly deep events in the southern Hikurangi margin, and predominantly shallow events in the northern region [*Wallace and Beavan*, 2010], particularly the Gisborne area where the first slow slip event was documented in October 2002 [*Douglas et al*., 2005]. To date, dozens of SSEs have been recorded in the same region within a depth range between 10 and 15 km. *Todd and Schwartz* [2016] recently published a catalogue of tectonic tremors for the northern Hikurangi Margin. They showed that most of the detectable tremors were accompanied with slow slip events, with frequent tremors observed in the Tokomaru Bay region in the northern Hikurangi, where cGPS observations show multiple short duration slow slip events. This pattern of shallow SSEs with short duration is clear in the GPS time series in the Tokomaru Bay region (Figures 2 and 3, PUKE) and extends along-strike toward the north of the margin. SSEs at the northern Hikurangi margin are typically associated with heightened levels of microseismicity, suggesting that SSEs trigger seismicity there [*Delahaye et al*., 2009]. An episode of SSE was observed during the 3 weeks period following the 2007 M_w 6.6 Gisborne earthquake also suggests that local earthquakes are capable of triggering SSEs at north Hikurangi [*François-Holden et al*., 2008].

In this study, we document four SSEs between June 2015 and September 2016. The first SSE in that period was in June 2015, located south of Tolaga Bay within a depth range between 9 and 15 km (Figure 3). We note that the depth ranges in the offshore region are somewhat uncertain due to the fact that we rely on onshore-based cGPS data for these inversions. This was the deepest event recorded in our study with an average slip of 15 mm; the deformation pattern suggests a hint of southward propagation toward Gisborne. This event is very comparable to the two SSEs reported by *Wallace and Beavan* [2010] in the same region in 2004 and 2008 and where tremors were reported in February–April 2015 [*Todd and Schwartz*, 2016].

In May 2016, the second SSE occurred south of the Tokomaru Bay region (and slightly to the north of the June 2015 event) with a maximum eastward displacement observed at PUKE (Figure 2). Our slip inversion resulted in a shallower depth range (6–12 km), compared to the 2015 event, with an average slip of 20 mm. A month later, another event occurred farther south, near Gisborne.

The June 2016 event has many similarities to the December 2007 SSE documented by *Wallace and Beavan* [2010], who proposed that this 2007 SSE was the result of triggering process by the M_w 6.6 Gisborne earthquake that occurred immediately prior to the SSE. The December 2007 SSE was followed by two SSEs in February and March 2008 in the Hawkes Bay and Mahia region. In contrast, the 2016 SSE sequence migration involved a northward migration of the SSE slip, and 2 months later, another SSE occurred in August 2016 in the Tolaga Bay and Tokomaru Bay regions (overlapping spatially with the May and June 2016 events a few months earlier) with an equivalent magnitude of 6.7. Nine days after the initiation of this event, the M_w 7.1 Te Araroa earthquake struck northeast of the ongoing SSE, ~50 km offshore of the Raukumara Peninsula. Ten days after the earthquake, we started to observe a deceleration toward the inter-SSE rate in the eastern component of GPS time series of most sites in Tokomaru Bay, Tolaga Bay, and Gisborne areas, with the

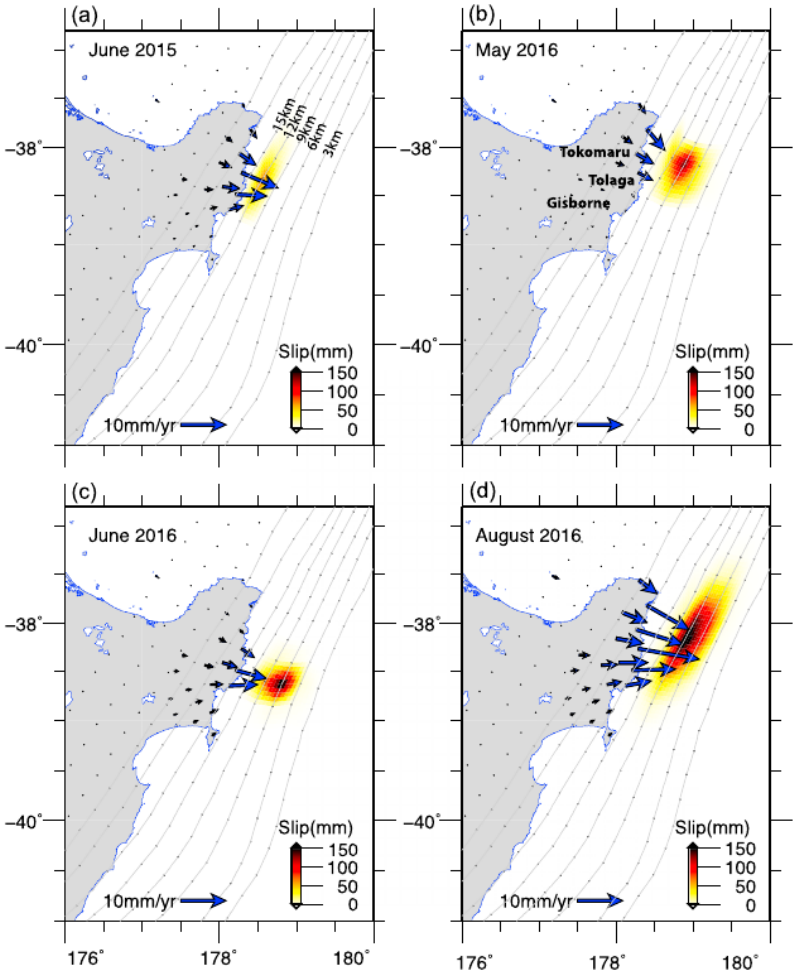

Figure 3. Slip distributions during each SSE (colors). The blue vectors show the associated predicted surface displacement. Gray lines and black dots correspond to the subduction depth contours (the labels are marked in the top left panel only for clarity).

exception of the site located in the Hicks Bay (HIKB), where an eastward acceleration began just after the earthquake, most likely related to an afterslip and/or slow slip on the subduction interface triggered by the M_w 7.1 earthquake. This slowing and subsequent cessation of the SSE after a 2 week duration at cGPS sites from Gisborne to Tokomaru Bay is typical of the duration of SSEs observed in this region previously [*Wallace et al*., 2012], and the deceleration is not necessarily related to the *M*7.1 earthquake. The proximity in time of the Tokomaru Bay SSE (late August 2016) just prior to the coseismic rupture suggests the possibility that the Te Araroa earthquake itself was triggered by the preceding SSE. Our observations of SSE deformation preceding and following the M_w 7.1 Te Araroa earthquake present an excellent example of a complex interplay between an SSE sequence and an earthquake. To gain more insight into this complex interaction between the Tokomaru Bay SSE and the Te Araroa earthquake, we will evaluate coulomb stress changes in the following section.

3.2. Coulomb Stress Changes Induced by the SSE and Earthquake

We have used the slip distribution for the Tokomaru Bay August 2016 SSE obtained from our TDefnode inversion to calculate the stress changes induced on the fault plane hosting the M_w 7.1 coseismic rupture (section 2.2). Coulomb stress changes (ΔCFS) were calculated using Coulomb 3.3 [*Lin and Stein*, 2004; *Toda et al*., 2005] using an effective coefficient of friction of 0.4. We obtain similar results using a higher

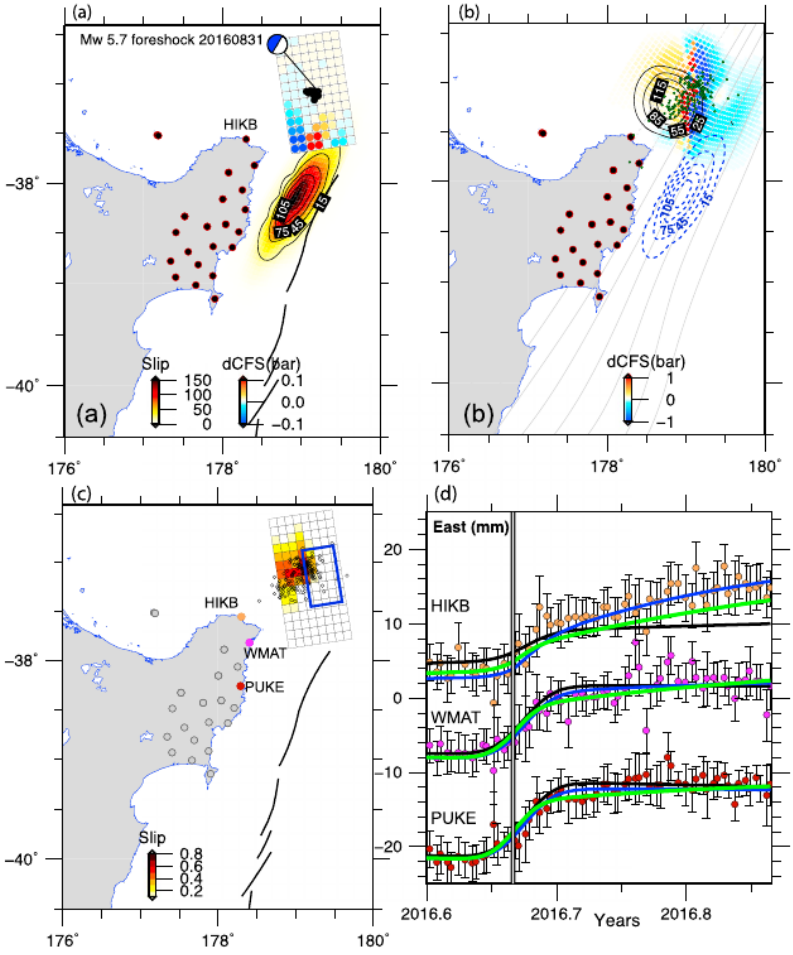

Figure 4. Coulomb stress change calculations for the (a) August 2016 SSE resolved on the earthquake fault rupture patches and for the (b) M_w 7.1 earthquake on the northern Hikurangi subduction interface; green circles in Figure 4b are the 1 day aftershocks of the earthquake (source: GeoNet catalogue); the black contours in Figure 4b refer to the postearthquake transient modeled on the subduction interface (scenario 2); blue dashed contours are the slip distribution of the August 2016 SSE (same as Figure 3d); (c) coseismic slip distribution inverted using W-phase. The solid blue rectangle delineate where afterslip was inverted (scenario 1); (d) comparison between the models fits of the two transient model scenarios; the blue line represents the model with a transient on the subduction slab interface, the green line shows the afterslip model on the bottom 20 km of the earthquake's modeled fault plane, and the black line is the model without including a transient after the earthquake.

coefficient of friction 0.6. Figure 4a shows ΔCFS resolved on each patch of the fault. The patches located on the middle part of the southern end of the fault show an increase up to 0.1 bar (0.01 MPa) (Figure 4a). Such small stress changes, around 0.01 MPa, are unlikely to trigger a large magnitude earthquake according to most of the cases reported in literature [*King et al.*, 1994; *Stein*, 1999]. The Te Araroa earthquake was preceded, 1 day before, by foreshock activity (in the 24 h prior to the earthquake) adjacent to the aftershock region (Figures 1 and 4a). Although it is plausible that the *M*7.1 earthquake was triggered by static stress changes induced by the SSE, the M_w 7.1 could likewise have been triggered by dynamic or static stress changes induced by the M_w 5.1 foreshock. Similarly, it is possible that the foreshock was triggered by the static stress perturbations imparted by the slow slip event. Although there was a roughly 1 day time lag between the foreshock and main shock, many studies have reported triggered seismicity delayed with seconds to weeks after the passage of the seismic wave [e.g., *Singh et al.*, 1998; *Hill and Prejean*, 2007]. We also cannot rule out possible involvement of secondary processes such as pore pressure increase due to fluid migration [e.g., *Noir et al.*, 1997; *Vidale and Shearer*, 2006], after the SSE and M_w 5.1

foreshock. The spatiotemporal migration of the May to August 2016 SSEs and the foreshock suggests a possible cascade of triggering, from SSEs through to the M_w 5.7 foreshock, and then the M_w 7.1 earthquake and its aftershock sequence. Although the static stress changes as well as the time lapse between the events do suggest the possibility of direct triggering of the M_w 7.1 by the SSE, it is possible that the SSEs kick started the foreshock sequence the day before the M_w 7.1 earthquake, which in turn led to the M_w 7.1. This situation is similar to other cases observed recently where several small foreshock swarms are collocated with slow slip occurring before the main shock rupture [*Kato et al*., 2012; *Walter et al*., 2015; *Socquet et al*., 2017].

Interestingly, the time series of the east component of the Hicks Bay cGPS site (HIKB) did not show a signal of rapid change after the earthquake. It showed however a slightly longer-lived transient (a few months) than what is typically seen in the area (a few weeks). Unfortunately, we could not track the long-term spatiotemporal variation of this transient because 2 months later the M_w 7.8 Kaikoura earthquake caused an offset in most of the sites in the Northern Island and trigged many SSEs along the Hikurangi margin [*Wallace et al*., in press]. The Te Araroa earthquake involved a normal faulting mechanism in the accretionary wedge with maximum slip occurred around a depth of 20 km, although the depth constraints on the earthquake are poor. The depth location of aftershocks is not well constrained and does not show a specific pattern which we could use to constrain the location of afterslip (or triggered slow slip) observed at site HIKB.

To evaluate the origin of the longer-lived postearthquake transient deformation observed at HIKB, we have calculated the ΔCFS imposed by the Te Araroa earthquake on the subduction interface at the northern Hikurangi margin, where the Tokomaru Bay SSE occurred (Figure 4b). The results show a reduction of the predicted ΔCFS by ~0.1 bar except in the most northern tip of the SSE patch where an increase is obtained. This is a very small change compared to what has been observed in the arrest of the Kapiti SSE by the 2014 Eketahuna [*Wallace et al*., 2014], suggesting that it is unlikely that the stress caused by the earthquake influenced the postearthquake slip behavior of the Tokomaru Bay SSE. However, the earthquake caused a pattern of the ΔCFS with a significant increase downdip and decrease updip of the megathrust plane where the rupture plane intersects with the subduction interface. This means that areas of the megathrust with positive coulomb stress are closer to failure and areas with negative values are inhibiting failure. The increase in ΔCFS up to ~10 bar, above the failure threshold of ~0.5 bar cited in *Lin and Stein* [2004], at the megathrust, suggests that transient observed in HIKB time series might be associated with a source on the critically stressed areas of the subduction interface and not necessarily on the downdip extent of the earthquake rupture plane [e.g., *Hsu et al*., 2002].

Two scenarios are considered to explain the long-lived transient after the earthquake: (i) Afterslip occurring on the normal fault plane responsible for the M_w 7.1 earthquake and (ii) a transient slip event on the subduction interface triggered by the earthquake (Figure 4d). We have tested both scenarios by (i) inverting for a transient on a uniform rectangular plane downdip of the coseismic rupture (the free parameters comprise a time constant, slip, rake, along-dip, and along-strike lengths) and (ii) by using a Gaussian slip patch (with similar parametrization as described in section 2.1) of the subduction interface. The results show that the second scenario better explains the decay in HIKB time series. The slip distribution associated with the postearthquake transient most likely on the subduction interface correlates well with areas of increased coulomb stress change (Figure 4b), suggesting that stress change induced by the main shock may have triggered a transient creep event on the northern Hikurangi megathrust section.

It is important to emphasize the limited resolution of the extent of the postearthquake transient signal observed at HIKB. The closest site to HIKB is within 30 km (WMAT) does not show a transient after the earthquake. The only way to fit this is by a transient deformation event located farther offshore and north of the August 2016 SSE (Figure 4d). HIKB has been operating since 2002, and there have been no previous large transient deformation events observed at that site since that time. If the postearthquake transient observed in the HIKB time series is indeed a slow slip event on the subduction interface, this represents the northernmost slow slip event ever observed at the Hikurangi margin.

4. Conclusion

In this study, we document a sequence of slow slip events in the northern Hikurangi margin. We show a complex situation of the interaction between SSE and earthquakes involving a possible foreshock and/or main

shock triggering by a northward propagating SSE, and afterslip, or triggered slow slip on the interface following the earthquake. The analysis of the continuous GPS time series shows SSEs farther to the northeast (affecting HIKB) than has been observed previously. The M_w 7.1 East Te Araroa earthquake and its foreshock may have been triggered by the cumulative effect of three, northward migrating slow slip events between May and August 2016. We document a long-lived transient beginning immediately after the M_w 7.1 earthquake observed in the eastern component of the site located in Hicks Bay. The limited spatial extent of the surface deformation associated with this transient suggests that this transient if located offshore, northeast of Hicks Bay, close enough to HIKB to be observed by that site, but too far offshore to be observed by other sites farther away (such as WMAT).

Observations of a SSE-earthquake-SSE/afterslip sequence have implications for our understanding of the interaction between SSEs and foreshock-main shock-aftershock sequences. Dense offshore geodetic and seismological observations are needed to better constrain the detailed interrelationships between shallow SSEs and large, potentially damaging earthquakes.

Acknowledgments
All seismic and GPS data used in this study are available from GeoNet (http://www.geonet.org.nz). HIKB and GISB cGPS sites are part of the PositioNZ network, run by GeoNet in collaboration with Land Information New Zealand. All figures were made with GMT. We thank the two anonymous reviewers for their insightful comments.

References

Araki, E., D. M. Saffer, A. J. Kopf, L. M. Wallace, T. Kimura, Y. Machida, et al. (2017), Recurring and triggered slow-slip events near the trench at the Nankai trough subduction megathrust, *Science*, *356*(6343), 1157.

Bartlow, N. M., L. M. Wallace, R. J. Beavan, S. Bannister, and P. Segall (2014), Time-dependent modeling of slow slip events and associated seismicity and tremor at the Hikurangi subduction zone, New Zealand, *J. Geophys. Res. Solid Earth*, *119*, 734–753, doi:10.1002/2013JB010609.

Benavente, R., and P. Cummins (2013), Simple and reliable finite fault solutions for large earthquakes using the W-phase: The Maule (M_w = 8.8) and Tohoku (M_w = 9.0) earthquakes, *Geophys. Res. Lett.*, *40*, 3591–3595, doi:10.1002/grl.50648.

Benavente, R., P. R. Cummins, and J. Dettmer (2016), Rapid automated W-phase slip inversion for the Illapel great earthquake (2015, M_w = 8.3), *Geophys. Res. Lett.*, *43*, 1910–1917, doi:10.1002/2015GL067418.

Delahaye, E. J., J. Townend, M. E. Reyners, and G. Rodgers (2009), Microseismicity but no tremor accompanying slow slip in the Hikurangi subduction zone, New Zealand, *Earth Planet. Sci. Lett.*, *277*, 21–28.

Dixon, T. H., Y. Jiang, R. Malservisi, R. McCaffrey, N. Voss, M. Protti, and V. Gonzalez (2014), Earthquake and tsunami forecasts: Relation of slow slip events to subsequent earthquake rupture, *Proc. Natl. Acad. Sci.*, *111*(48), 17039–17044.

Doser, D. I., and T. H. Webb (2003), Source parameters of large historical (1917–1961) earthquakes, North Island, New Zealand, *Geophys. J. Int.*, *152*, 795–832.

Douglas, A., J. Beavan, L. Wallace, and J. Townend (2005), Slow slip on the northern Hikurangi subduction interface, New Zealand, *Geophys. Res. Lett.*, *32*, L16305, doi:10.1029/2005GL023607.

Dragert, H., K. Wang, and T. James (2001), A silent slip event on the deeper Cascadia subduction interface, *Science*, *292*, 1525–1528.

François-Holden, C., et al. (2008), The M_w 6.6 Gisborne earthquake of 2007: Preliminary records and general source characterization, *Bull. N. Z. Soc. Earthquake Eng.*, *41*(4), 266–277.

Hill, D. P., and S. G. Prejean (2007), 4.09 - Dynamic triggering, in *Treatise on Geophysics*, edited by G. Schubert, pp. 257–291, Elsevier, Amsterdam.

Hsu, Y. J., N. Bechor, P. Segall, S. B. Yu, L. C. Kuo, and K. F. Ma (2002), Rapid afterslip following the 1999 Chi-Chi, Taiwan earthquake, *Geophys. Res. Lett.*, *29*(16), 1–4, L15S12, doi:10.1029/2002GL014967.

Ito, Y., K. Obara, K. Shiomi, S. Sekine, and H. Hirose (2007), Slow earthquakes coincident with episodic tremors and slow slip events, *Science*, *315*(5811), 503–506.

Kato, A., K. Obara, T. Igarashi, H. Tsuruoka, S. Nakagawa, and N. Hirata (2012), Propagation of slow slip leading up to the 2011 M_w 9.0 Tohoku-Oki earthquake, *Science*, *335*, 705–708.

King, G. C. P., R. S. Stein, and J. Lin (1994), Static stress changes and the triggering of earthquakes, *Bull. Seismol. Soc. Am.*, *84*(3), 935–953.

Lin, J., and R. S. Stein (2004), Stress triggering in thrust and subduction earthquakes and stress interaction between the southern San Andreas and nearby thrust and strike-slip faults, *J. Geophys. Res.*, *109*, B02303, doi:10.1029/2003JB002607.

McCaffrey, R. (2009), Time-dependent inversion of three-component continuous GPS for steady and transient sources in northern Cascadia, *Geophys. Res. Lett.*, *36*, L07304, doi:10.1029/2008GL036784.

McCaffrey, R. (2014), Interseismic locking on the Hikurangi subduction zone: Uncertainties from slow-slip events, *J. Geophys. Res. Solid Earth*, *119*, 7874–7888, doi:10.1002/2014JB010945.

Noir, J., E. Jacques, S. Bekri, P. M. Adler, P. Tapponier, and G. C. P. King (1997), Fluid flow triggered migration of events in the 1989 Dobi earthquake sequence of central afar, *Geophys. Res. Lett.*, *24*, 2335–2338.

Ozawa, S., H. Suito, and M. Tobita (2007), Occurrence of quasi-periodic slow-slip off the east coast of the Boso peninsula, central Japan, *Earth Planets Space*, *59*, 1241–1245.

Peng, Z., and J. Gomberg (2010), An integrated perspective of the continuum between earthquakes and slow-slip phenomena, *Nat. Geosci.*, *3*, 599–607.

Press, W. H., B. P. Flannery, S. A. Teukolsky, and W. T. Vetterling (1989), *Numerical Recipes*, Cambridge Univ. Press, New York.

Radiguet, M., H. Perfettini, N. Cotte, A. Gualandi, B. Valette, V. Kostoglodov, T. Lhomme, A. Walpersdorf, E. Cabral Cano, and M. Campillo (2016), triggering of the 2014 M_w7.3 Papanoa earthquake by a slow slip event in Guerrero, Mexico, *Nat. Geosci.*, doi:10.1038/ngeo2817.

Saffer, D. M., and L. M. Wallace (2015), The frictional, hydrologic, metamorphic and thermal habitat of shallow slow earthquakes, *Nat. Geosci.*, *8*, 594–600.

Schwartz, S. Y., and J. M. Rokosky (2007), Slow slip events and seismic tremor at circum Pacific subduction zones, *Rev. Geophys.*, *45*, RG3004, doi:10.1029/2006RG000208.

Segall, P., and A. M. Bradley (2012), Slow-slip evolves into megathrust earthquakes in 2D numerical simulations, *Geophys. Res. Lett.*, *39*, L18308, doi:10.1029/2012GL052811.

Segall, P., E. K. Desmarais, D. Shelly, A. Mikilius, and P. Cervelli (2006), Earthquakes triggered by silent slip events on Kilauea volcano, Hawaii, *Nature*, *442*, 71–74.

Singh, S. K., J. G. Anderson, and M. Rodriguez (1998), Triggered seismicity in the Valley of Mexico from major Mexican earthquakes, *Geofis. Int.*, *37*, 3–15.

Socquet, A., J. P. Valdes, J. Jara, F. Cotton, A. Walpersdorf, N. Cotte, S. Specht, F. Ortega-Culaciati, D. Carrizo, and E. Norabuena (2017), An 8 month slow slip event triggers progressive nucleation of the 2014 Chile megathrust, *Geophys. Res. Lett.*, *44*, 4046–4053, doi:10.1002/2017GL073023.

Stein, R. S. (1999), The role of stress transfer in earthquake occurrence, *Nature*, *402*(6762), 605–609.

Toda, S., R. S. Stein, K. Richards-Dinger, and S. Bozkurt (2005), Forecasting the evolution of seismicity in southern California: Animations built on earthquake stress transfer, *J. Geophys. Res.*, *110*, B05S16, doi:10.1029/2004JB003415.

Todd, E. K., and S. Y. Schwartz (2016), Tectonic tremor along the northern Hikurangi margin, New Zealand, between 2010 and 2015, *J. Geophys. Res. Solid Earth*, *121*, 8706–8719, doi:10.1002/2016JB013480.

Vallée, M., et al. (2013), Intense interface seismicity triggered by a shallow slow slip event in the Central Ecuador subduction zone, *J. Geophys. Res. Solid Earth*, *118*, 2965–2981, doi:10.1002/jgrb.50216.

Vidale, J. E., and P. M. Shearer (2006), A survey of 71 earthquake bursts across southern California: Exploring the role of pore fluid pressure fluctuations and aseismic slip as drivers, *J. Geophys. Res.*, *111*, B05312, doi:10.1029/2005JB004034.

Wallace, L. M., and J. Beavan (2010), Diverse slow slip behavior at the Hikurangi subduction margin, New Zealand, *J. Geophys. Res.*, *115*, B12402, doi:10.1029/2010JB007717.

Wallace, L. M., P. Barnes, J. Beavan, R. Van Dissen, N. Litchfield, J. Mountjoy, R. Langridge, G. Lamarche, and N. Pondard (2012), The kinematics of a transition from subduction to strike-slip: An example from the central New Zealand plate boundary, *J. Geophys. Res.*, *117*, B02405, doi:10.1029/2011JB008640.

Wallace, L. M., N. Bartlow, I. Hamling, and B. Fry (2014), Quake clamps down on slow slip, *Geophys. Res. Lett.*, *41*, 8840–8846, doi:10.1002/2014GL062367.

Wallace, L. M., S. C. Webb, Y. Ito, K. Mochizuki, R. Hino, S. Henrys, et al. (2016), Slow slip near the trench at the Hikurangi subduction zone, New Zealand, *Science*, *352*(6286), 701–704.

Wallace, L. M., Y. Kaneko, S. Hreinsdottir, I. Hamling, Z. Peng, N. Bartlow, E. D'Anastasio, and B. Fry (in press), Large-scale dynamic triggering of shallow slow slip enhanced by overlying sedimentary wedge, Nature Geoscience, in press, doi:10.1038/ngeo3021.

Walter, J. I., X. Meng, Z. Peng, S. Y. Schwartz, A. V. Newman, and M. Protti (2015), Far-field triggering of foreshocks near the nucleation zone of the 5 September 2012 (Mw 7.6) Nicoya Peninsula, Costa Rica earthquake, *Earth Planet. Sci. Lett.*, *431*, 75–86.

Williams, C. A., D. Eberhart-Phillips, S. Bannister, D. H. N. Barker, S. Henrys, M. Reyners, and R. Sutherland (2013), Revised interface geometry for the Hikurangi subduction zone, New Zealand, *Seismol. Res. Lett.*, *84*(6), 1066–1073.

Yoshimoto, M., and Y. Yamanaka (2014), Teleseismic inversion of the 2004 Sumatra-Andaman earthquake rupture process using complete Green's functions, *Earth Planets Space*, *66*(1), 152, doi:10.1186/s40623-014-0152-4.